

Deep Residual Networks for Sleep Posture Recognition With Unobtrusive Miniature Scale Smart Mat System

Haikang Diao , Chen Chen , Wei Yuan , Amara Amara, Toshiyo Tamura , Jiahao Fan , Long Meng , Xiangyu Liu, and Wei Chen , *Senior Member, IEEE*

Abstract—Sleep posture, as a crucial index for sleep quality assessment, has been widely studied in sleep analysis. In this paper, an unobtrusive smart mat system based on a dense flexible sensor array and printed electrodes along with an algorithmic framework for sleep posture recognition is proposed. With the dense flexible sensor array, the system offers a comfortable and high-resolution solution for long-term pressure sensing. Meanwhile, compared to other methods, it reduces production costs and computational complexity with a smaller area of the mat and improves portability with fewer sensors. To distinguish the sleep posture, the algorithmic framework that includes preprocessing and Deep Residual Networks (ResNet) is developed. With the ResNet, the proposed system can omit the complex hand-crafted feature extraction process and provide compelling performance. The feasibility and reliability of

the proposed system were evaluated on seventeen subjects. Experimental results exhibit that the accuracy of the short-term test is up to 95.08% and the overnight sleep study is up to 86.35% for four categories (supine, prone, right, and left) classification, which outperform the most of state-of-the-art studies. With the promising results, the proposed system showed great potential in applications like sleep studies, prevention of pressure ulcers, etc.

Index Terms—Sleep posture recognition, smart mat system, unobtrusive monitoring, ResNet.

I. INTRODUCTION

PEOPLE spend one-third of their time to sleep. Good sleep could improve work efficiency, strengthen the immunity system, maintain physical fitness, etc. People with poor sleep quality may be prone to feel extremely fatigued and emotionally exhausted [1], [2]. Sleep posture, as an essential index for sleep analysis, has been extensively investigated in sleep monitoring and the healthcare of long-term bedridden patients. Wrong sleep posture may exacerbate airflow obstruction and contribute to increased arousal and sleep disturbance like sleep apnea [3]–[5]; increase the burden of muscles and ligaments and result in shoulder, neck, or back pain; or even affect the blood circulation and induce pressure ulcers [6]. Pressure ulcers, as a serious disease caused by remaining on the same posture for a long time, which breaks down the skin and underlying tissue, may encounter in bedridden patients [7], [8]. In the world, approximately 60000 people die from complications of pressure injuries every year. Individuals with pressure ulcers have a 4.5-times greater risk of death than persons with the same risk factors but without pressure injuries. Thus, long-term monitoring and early prevention of wrong sleep postures towards exacerbation events like sleep apnea or pressure ulcer are extremely important.

To provide comprehensive information on continuous postures tracking and to relieve the burden of the caregivers of bedridden patients, automatic sleep posture recognition methods have been extensively investigated. These methods can be roughly classified into two categories. The first category is the camera-based method. Video cameras [9] and near-infrared cameras [10], [11] have been used to record and monitor the sleep postures through image information. However, this method is sensitive to occlusion arise from a blanket or changes in environmental illumination. Meantime, it may raise privacy concerns or even lead to privacy leakage. The second category

Manuscript received October 26, 2020; revised December 15, 2020; accepted January 7, 2021. Date of publication January 22, 2021; date of current version March 30, 2021. This work was supported in part by National Key R&D Program of China under Grant 2017YFE0112000, in part by Shanghai Municipal Science and Technology Major Project under Grant 2017SHZDZX01, in part by Shanghai Municipal Science and Technology International R&D Collaboration Project under Grant 20510710500, in part by the National Natural Science Foundation of China under Grant 62001118, and in part by the Shanghai Committee of Science and Technology under Grant 20S31903900. (*Corresponding authors:* Chen Chen; Wei Chen.)

Haikang Diao, Jiahao Fan, and Long Meng are with the Center for Intelligent Medical Electronics, School of Information Science and Technology, Fudan University, Shanghai 200433, China (e-mail: 19210720023@fudan.edu.cn; 18110720059@fudan.edu.cn; lmeng18@fudan.edu.cn).

Chen Chen is with the Center for Intelligent Medical Electronics, School of Information Science and Technology, Fudan University, Shanghai 200433, China, and also with the Human Phenome Institute, Fudan University, Shanghai 201203, China (e-mail: chenchenfd@fudan.edu.cn).

Wei Yuan is with the Printable Electronics Research Centre, Suzhou Institute of Nanotech and Nano-Bionics, Chinese Academy of Sciences, Suzhou 215123, China (e-mail: wyuan2014@sinano.ac.cn).

Amara Amara is with the Terre des Hommes Foundation, Paris 75006, France (e-mail: amara.amara@tdh.ch).

Toshiyo Tamura is with the Japanese Society of Medical Electronics and Biological Engineering, Japanese Society of Life Support Technology, and Japanese Society for Nursing Science and Engineering, Tokyo 169-8050, Japan (e-mail: t.tamura1949@gmail.com).

Xiangyu Liu is with the Center for Intelligent Medical Electronics, School of Information Science and Technology, Fudan University, Shanghai 200433, China, and also with the East China University of Science and Technology, School of Art Design and Media, Shanghai 200237, China (e-mail: y12170017@mail.ecust.edu.cn).

Wei Chen is with the Center for Intelligent Medical Electronics, School of Information Science and Technology, Fudan University, Shanghai 200433, China, and also with the Human Phenome Institute, Fudan University, Shanghai 201203, China (e-mail: w_chen@fudan.edu.cn).

Color versions of one or more figures in this article are available at <https://doi.org/10.1109/TBCAS.2021.3053602>.

Digital Object Identifier 10.1109/TBCAS.2021.3053602

is to use a variety of wearable sensors [12], [13], such as triaxial accelerometers and gyroscopes. For example, several triaxial accelerometers are attached to human limbs, and sleep patterns are monitored by actigraph [14]. With the attached sensors, natural sleep may be disrupted. Moreover, signals acquired by this method are susceptible to motion artifacts, which may affect the accuracy of the sleep postures recognition.

Recently, as an alternative method, smart mat systems for unobtrusive sleep posture recognition attracted widespread attention. A large number of force-sensing resistors (FSR) are embedded in the mat to acquire the pressure distribution of the human body and machine learning methods are applied to classify the sleep postures. It provides a non-intrusive and comfortable way to recognize sleep postures without affecting natural sleep. Among existing smart mat systems, most of the studies use a low-density pressure sensor array that is uniformly distributed in the mat [15]–[17]. For example, there are only 4 sensors are distributed around the bed in [15], and the performance is related to the position of the person. A sensor pillow system which is equipped with 9 sensors was proposed in [16]. It requires people to put their arms on the pillow while sleeping to recognize different postures, and too few sensors cannot get pressure distribution accurately. [17] also proposed a sensor pillow system similar to [16], so it also has the same problems as [16]. Therefore, low-density pressure sensors array result in low-resolution of the image acquired from the pressure distribution, and further lead to a poor sleep postures classification accuracy. In contrast, some studies propose to use a high-resolution sensor array such as 2048 sensors or even 8196 sensors [18]–[20]. For instance, a smart mat with 1728 pressure sensors was proposed in [18], and the area of the mat is 1.41 m^2 . Similarly, [19] proposed a 1.62 m^2 smart mat with 2048 pressure sensors and [20] proposed a 1.5 m^2 smart mat with 2048 pressure sensors. These methods achieve high posture classification accuracy. However, the production cost and computational complexity are significantly increased. To date, existing research is focusing on using spare or dense sensors that are deployed on the whole mat to capture a sketch map of whole-body pressure distribution. It ignores that the deployed sensors across the whole mat may contribute to redundant information in dealing with pressure images and potentially increase the computational complexity. Meanwhile, partial sensors may not be used during the whole monitoring process, which may cause extravagance of sensors. Whether a miniature scale smart mat with deployed sensors or a mat with a limited area of deployed sensors is sufficient to provide adequate information in achieving satisfactory performance for sleep posture recognition needed to be further investigated.

In this paper, a smart mat with an area of $55 \text{ cm} \times 55 \text{ cm}$ and 1024 dispersed flexible sensors is presented. The mat can offer an unobtrusive, comfortable solution for long-term pressure sensing. After sensing pressure, an algorithmic framework that includes the pre-processing and Deep Residual Networks is proposed. To verify the feasibility of the proposed system, two sets of experiments, which are short-term and overnight experiments respectively, were conducted. The contributions of this paper can be summarized as follows:

1. A miniature scale smart mat system to provide a portable, non-intrusive, and comfortable way to identify the sleep

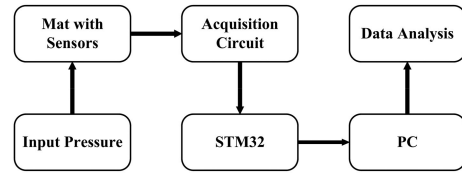


Fig. 1. The framework of the system.

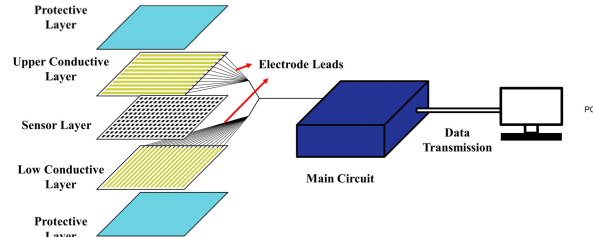


Fig. 2. Five-layer structure of the mat.

postures is designed. The proposed mat system can obtain the pressure distribution of major regions like the chest, part of the shoulders, and part of the hips efficiently, which can provide adequate information in achieving favorable performance for sleep posture recognition by taking the production costs, computational complexity, and portability into consideration.

2. The neural network ResNet, which doesn't require the complex hand-crafted feature extraction process, is proposed to recognize sleep postures. It is able to achieve compelling performance and enables real-time monitoring on a low-power embedded computing platform.
3. Overnight experiment was conducted to verify the feasibility of the system in a real scenario, which demonstrated the practical potential utilization of the proposed system.

The rest of the paper is organized as follows: Section II describes the system design and implementation. Section III presents the algorithm framework for sleep posture recognition. Section IV presents the experiment and the obtained results. Finally, the discussion and conclusion are given in Section V and Section VI respectively.

II. SYSTEM DESIGN AND IMPLEMENTATION

In this section, the sleep posture monitoring system is introduced. Followed by a detailed explanation of the mat design and system implementation.

The framework of the system is proposed in Fig. 1. The mat is used to convert the pressure distribution into a voltage signal. The acquisition circuits are used for signal control and acquisition, then the STM32 module is used to control the data acquisition process and send the data to the PC. Finally, the data is sent to the PC for further analysis, like sleep posture recognition.

A. The Mat Design

The mat is a five-layer structure with a thickness of 2 mm and an area of $55 \text{ cm} \times 55 \text{ cm}$, as shown in Fig. 2. It can cover the entire chest, part of the shoulders, and part of the hips.

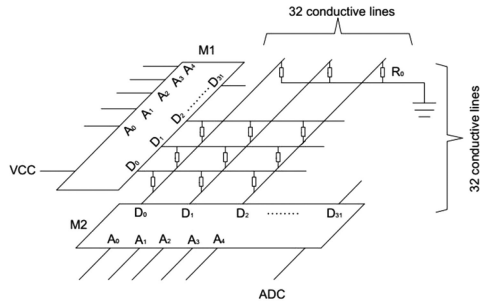


Fig. 3. Schematic of the smart mat system.

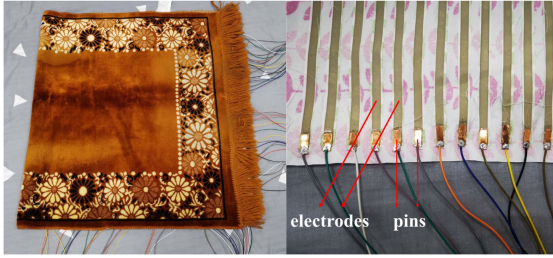


Fig. 4. Smart mat and electrodes.



Fig. 5. The force sensing resistor based on Velostat.

The protective layer is based on soft fabric. The conductive layer is made of 32 parallel strip printed electrodes. The interval between the electrodes is 0.8 cm, and the width of the electrodes is 1 cm. The upper and lower conductive layers are placed opposite each other in the horizontal and vertical directions. The schematic of the mat is presented in Fig. 3. Each electrode is connected to each pin, and the resistance from the electrode to the pin is 40Ω , which is much smaller than the resistance of the sensor, so it will not affect the performance of the mat. The smart mat and electrodes are presented in Fig. 4.

The sensor layer is located in the middle to form a $32 * 32$ pressure sensor array. It is made of flexible material based on Velostat. Velostat is one of the most common and low-priced materials in the force-sensing resistor (FSR) as Fig. 5 shows. FSR is an analog sensor that resistance changes with pressure. Its physical characteristics are that the initial resistance value is very high, and the resistance decreases sharply with increasing pressure. Its volume resistivity is up to $500 \Omega \cdot \text{cm}$, and surface resistivity is up to 31000Ω .

B. Data Acquisition Circuits

As Fig. 6 shows, the data acquisition circuit includes two circuits that are used for acquisition and signal control respectively.

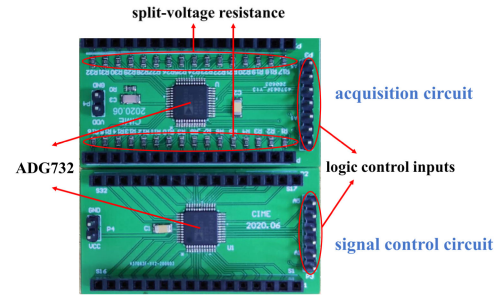


Fig. 6. Data acquisition circuit (the acquisition circuit is on the top, and the signal control circuit is on the bottom).

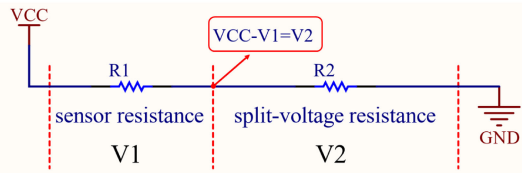


Fig. 7. Schematic of the circuit.

The acquisition circuit includes 32-channel analog multiplexers (ADG732) and 32 split-voltage resistance. The voltage value of each of the 32 pins can be obtained separately with ADG732. The signal control circuit supplies 3.3 V to 32 pins in turn with ADG732.

The schematic of the smart mat system is presented in Fig. 3. The upper conductive layer is connected to the signal control circuit, meanwhile, the lower conductive layer is connected to the acquisition circuit. Suppose the resistance value of the sensor is R_1 and the resistance value of the split-voltage resistor is R_2 . When the signal control circuit supplies 3.3 V voltage to one electrode, the voltage of the sensor is V_1 , and the voltage of the split-voltage resistance is V_2 . Fig. 7 presents that the voltage at the midpoint between the sensor and the split-voltage resistance is V_2 , so the relationship between R_1 and V_2 is:

$$R_1 = \left(\frac{3.3}{V_2} - 1 \right) R_2 \quad (1)$$

It can be concluded that R_1 is inversely proportional to V_2 , and the pressure is also inversely proportional to R_1 , so the pressure is proportional to V_2 . Therefore, the pressure value can be obtained by V_2 .

C. STM32 Module

The STM32 module is used to control the data acquisition process and send the data to the PC. It consists of a micro-unit (MCU), a UART model, a microSD card slot, and a 12-bit analog-to-digital converter (ADC) which is used for voltage conversion. The ADC range of the STM32 module is 0 to 3.3 V. The STM32 module controls the acquisition circuit and signal control circuit by connecting the logic control inputs of ADG732 as Fig. 6 shows.

The signal control circuit supplies 3.3 V to the 32 electrodes on the upper conductive layer in order from 1 to 32. When an electrode is high, the acquisition circuit transmits the voltage of

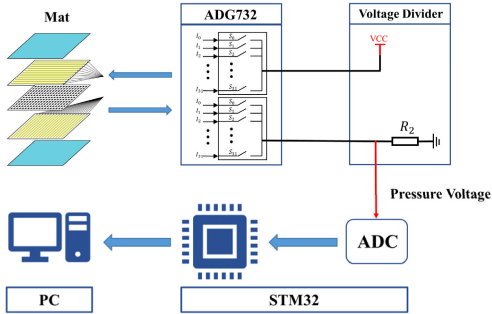


Fig. 8. Data acquisition process and system architecture.

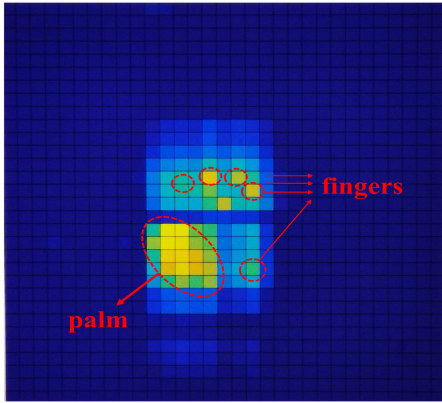


Fig. 9. Pressure distribution image when one hand is pressed on the mat.

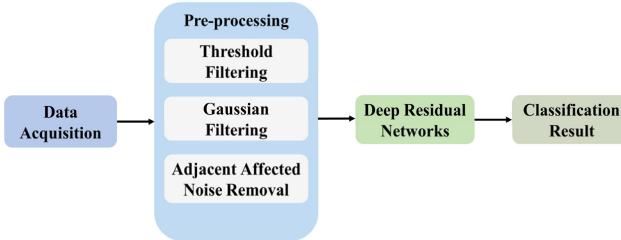


Fig. 10. Algorithmic framework for sleep posture recognition.

the 32 electrodes on the lower conductive layer to the ADC in sequence [10], then the ADC converts the voltage into a value. Therefore, the system reads a total of 1024 points of pressure information from the mat. As introduced in previous research [21], the system works similarly to matrix keyboard scanning, which reads the pressure value of each point in turn.

Fig. 8 summarizes the data acquisition process and system architecture. The pressure distribution image when one hand is pressed on the mat is shown in Fig. 9. We can clearly see the pressure distribution in the center of the image, even find the position of the palm and fingers.

III. ALGORITHM FOR SLEEP POSTURE CLASSIFICATION

In this section, an algorithmic framework for sleep posture recognition is proposed. Fig. 10 shows that the algorithm consists of two steps: pre-processing and Deep Residual Networks (ResNet) for posture classification. Sleep postures are classified into four categories: supine, prone, right, and left.

A. Pre-Processing

Pre-processing of the raw image is to remove noise and adjacent affected areas on the mat. The mattress is soft, so the sensor points pressed may affect the sensor points that are not pressed. Adjacent affected noise removal is to clear the redundant information in the raw images.

Firstly, because the ADC in our system is very sensitive, the subtle internal noise of the system will interfere with the pressure value acquired by the ADC even when sensors are not under pressure. Thus, Threshold Filtering is applied to remove this noise and eliminate system errors. The raw images are filtered with a threshold. Suppose the pressure value of each sensor in the raw image is $a_{i,j}$ ($1 \leq i \leq 32, 1 \leq j \leq 32$), The threshold filtering is defined as follows:

$$a_{i,j} = \begin{cases} a_{i,j} & a_{i,j} \geq Thre \\ 0 & \text{otherwise} \end{cases}$$

$$Thre = \frac{\sum_{i=1}^{32} \sum_{j=1}^{32} a_{i,j}}{1024} \quad (2)$$

Secondly, due to the movement of the subjects and changes in temperature, the acquired pressure images may contaminate with high-frequency noise and result in a reduced signal-to-noise ratio of the images. Gaussian filter is a non-uniform low pass filter and is more effective at smoothing images and removing the high-frequency noise. It has been widely used in the image processing domain. Therefore, to obtain the pressure distribution image with a higher signal-to-noise ratio, the Gaussian filter is applied.

Thirdly, the pressure sensors embedded in the mat are ultra-thin, flexible, and also sensitive to subtle deformation. When a subject lies down, the pressure on the part of the mat that is in contact with the body will change, but the pressure of the area that is not pressed by the body will also change slightly caused by deformation. Therefore, the Adjacent Affected Noise Removal is applied to remove redundant information.

Meanwhile, all the sensors in a column are often pressed by the body because the subject is lying on the mat from top to bottom, so there is no redundant information. And only a part of the sensors in a row is pressed by the body, it is necessary to calculate the local maximum value for a row of data and remove the redundant information for every row. If the local maximum value for a row of data is p_i (there may be several local maximum), the adjacent affected noise removal is defined as follows:

$$a_{i,j} = \begin{cases} a_{i,j} & a_{i,j} \geq Athre \\ 0 & \text{otherwise} \end{cases}$$

$$Athre = \frac{3}{4} * \min \{p_i\} \quad (3)$$

The reason why the threshold is not the minimum value of p_i is that another pressure value around the local maximum value needs to be preserved. Fig. 11 shows two pseudo-color images before and after pre-processing in a supine posture (The mat was placed between the subject's neck and hips. The neck corresponds to the top of the image, and the hips correspond to the bottom of the image). The redundant information is

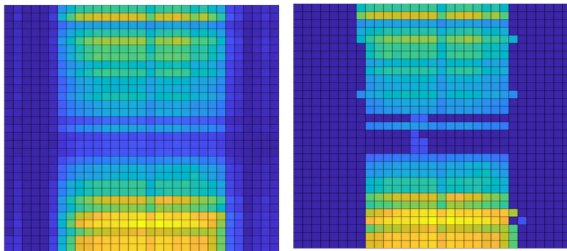


Fig. 11. Illustrations of pressure distribution images before and after pre-processing in a supine position (Left is before processing, and right is after processing).

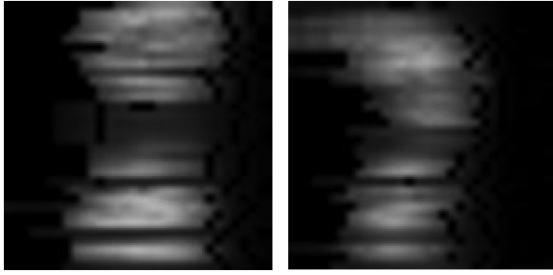


Fig. 12. Illustrations of pressure distribution images after converting into grayscale images (Left is before supine, and right is right).

removed and the image of pressure value becomes compact, which can extract features more accurately. Finally, the pressure distribution is converted into 160×160 grayscale images as Fig. 12 shows.

B. Deep Residual Networks (ResNet)

Convolutional Neural Networks (CNN) is a feed-forward neural network, and it has a good effect on image recognition. Especially, it reduces the complexity and size of the model compared to Deep Neural Networks (DNN). The Deep Residual Networks (ResNet) was proposed by He *et al.* in 2015 [22], which is one of the most commonly CNN. Theoretically, increasing the number of network layers should increase the representation capacity of the network and improve classification accuracy. However, in practice, this is not the case due to gradient disappearance and explosion. ResNet can solve this problem efficiently through residual blocks, thereby greatly increasing the number of network layers. Meanwhile, ResNet accelerates the speed of training of the deep networks. Instead of widening the network, ResNet increases the depth of the network results in fewer extra parameters. ResNet has obtained higher accuracy in network performance especially in image classification. He *et al.* showed that the ResNet perform better in image classification than other CNN models in the ImageNet dataset in 2015. Considering that the data set contains fewer samples, ResNet-18 is applied for sleep posture classification.

1) *CNN*: As Fig. 13 shows, the classic CNN is composed of an input layer, convolution layers, pooling layers, fully connected layers, and an output layer. The convolution layer is the most important feature of CNN. The convolution kernel scans the input image and performs convolution with the input image to extract the feature information of the local area. After

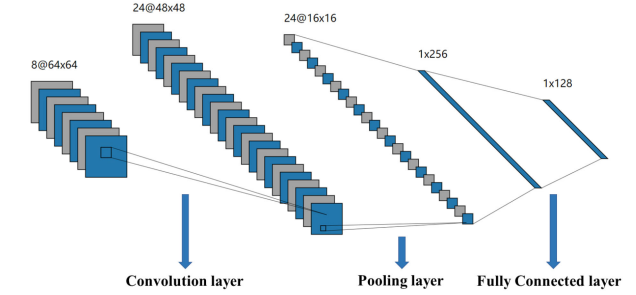


Fig. 13. Overall structure of the convolutional neural network.

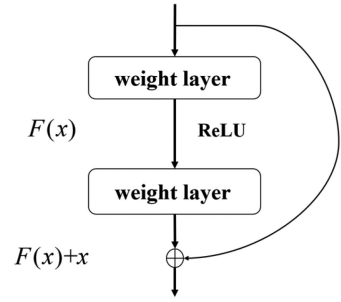


Fig. 14. Residual unit structure diagram.

activation by the active function, a new feature map of the image is obtained. The convolution operation can be described by the following formula:

$$X_j^{l+1} = f \left(\sum_{i \in M_j} x_i^l * k_{i,j}^{l+1} + b_j^l \right) \quad (4)$$

X_j^l denotes the j th feature map of the l th convolution layer, which also is the input of the current layer. X_j^{l+1} denotes the j th feature map of the $(l+1)$ th convolution layer. M denotes a set of input feature maps, $*$ denotes a convolution operation, k denotes a convolution kernel, b denotes the bias, and f denotes the active function.

The pooling layer is used to reduce the size of the feature map by down-sampling. The common methods include average pooling, maximum pooling, and L_p pooling. Maximum pooling is widely used because of its simple operation and high efficiency. The fully connected layer is used to obtain the classification results.

2) *Resnet*: Fig. 14 shows the residual block, which is the core of the ResNet model. The residual block is defined as:

$$y = F(x, \{W_i\}) + x \quad (5)$$

$$F = W_2 \sigma(W_1 x) = y - x \quad (6)$$

where x and y are the input and output of the current layer. W_1 and W_2 represent the weights of the first and second layers respectively, and σ denotes the ReLU function. The function $F(x, \{W_i\})$ represents the residual mapping to be learned. The shortcut connections in the residual block allow the sub-module directly to learn makes the target output become $F + x$.

As Fig. 15 shows, the ResNet-18 model consists of 17 convolution layers, 2 pooling layers, 8 residual units, and 3 fully

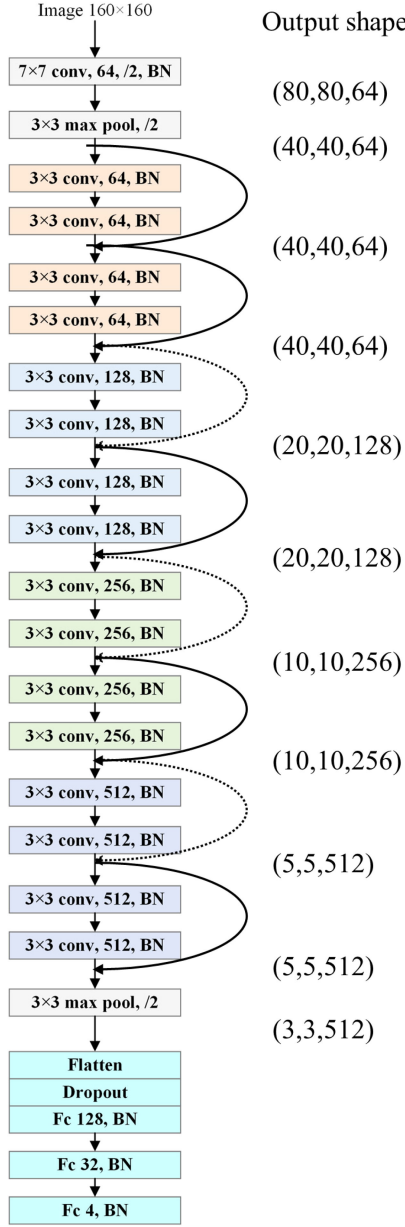


Fig. 15. Network structure of ResNet-18.

connected layers. Different from the classic ResNet-18 structure, we have added Batch Normalization (BN) layer after each convolution layer. BN layer normalizes layer outputs by making it have the mean of zero and the variance of 1. Meanwhile, the BN layer stabilizes the learning process and dramatically reduces the number of training epochs required to train deep networks. The BN operation can be described by the following formula:

$$u_B = \frac{1}{m} \sum_{i=1}^m x_i, \sigma_B^2 = \frac{1}{m} \sum_{i=1}^m (x_i - u_B)^2 \quad (7)$$

$$x_i^* = \frac{x_i - u_B}{\sqrt{\sigma_B^2 + \varepsilon}}, y_i = \gamma x_i^* + \beta \quad (8)$$

$B = \{x_1, x_2, \dots, x_m\}$, and it denotes one batch of input. u_B denotes the mean of the batch, and σ_B^2 denotes the variance

TABLE I
SUBJECTS INFORMATION AND CLASSIFICATION ACCURACY

	Gender	Age	Height (cm)	Weight (kg)	The Number of the samples	accuracy
1	Female	23	158	55	59	100%
2	Male	31	178	76.5	72	88.89%
3	Male	22	171	76	72	94.44%
4	Male	26	170	65	72	97.22%
5	Female	24	168	50	68	91.18%
6	Male	25	175	60	72	97.22%
7	Female	23	158	48	72	97.22%
8	Male	24	171	70	71	91.67%
9	Female	28	165	52	69	100%
10	Female	29	160	51	72	98.61%
11	Male	25	173	75	72	100%
12	Male	29	175	83	60	100%
13	Male	23	180	70	72	100%
14	Female	26	170	54	69	100%
15	Female	28	160	50	45	93.33%
16	Male	33	174	75	39	84.62%

of the batch. u_B and σ_B^2 are calculated directly in the forward propagation. ε is to prevent the situation where $\sigma_B^2 = 0$. γ and β are trained in the backpropagation.

IV. EXPERIMENT AND RESULTS

In this section, the experimental setup and experimental results are introduced. Two sets of experiments namely short-term experiment and long-term experiment are conducted to evaluate the feasibility and reliability of the system for sleep posture recognition.

A. Experimental Setup

We conducted two sets of experiments to evaluate the performance of the system for sleep posture recognition. The first experiment was a short-term experiment to evaluate the feasibility of the proposed system. It was worth noting that the data collected in this experiment are all short-term and fixed-interval. Each posture was held for 20 seconds, and the interval between the two postures was 15 seconds. The sampling rate is 9 Hz, and about 2 or 3 samples are saved within 20 seconds. The number of samples for each subject is shown in Table I. In order to simulate the real scene, the subjects can move slightly during the experiment. Some subjects may move significantly during the experiment, then these samples will be discarded. Therefore, the number of samples for each subject is different. The second experiment was to evaluate the performance of the system in a real scenario by collecting data throughout the night. The results of the second experiment are given in Section C.

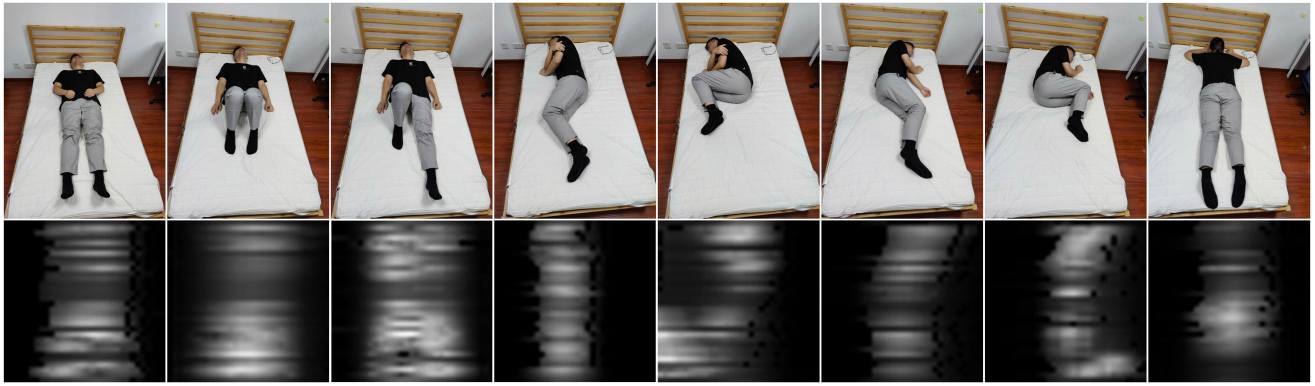


Fig. 16. (a) Examples of 8 postures; (b) The illustration of pressure distribution images corresponds to the examples.

Sixteen subjects (9 males, 7 females) were included in the sleep posture recognition experiment. Table I shows the details of the subjects. The height of the subjects ranged from 158 to 180 cm, and the weight ranged from 48 to 83 kilograms. The written consent was acquired from each participant before the experimental sessions. The mat was placed between the subject's neck and hips to record the pressure distribution.

Lying on the left and right sides with legs bent while sleeping are most common at 41% according to Idzikowski's study [23], and other side-lying postures with straight legs account for 28%. It can be seen that even in the same side-lying posture, there are at least two common postures (bent legs or straight legs). Therefore, although all postures were only divided into four categories (supine, prone, right, and left), it was necessary to acquire as many categories as possible during the experiment. After investigation, we acquired 8 postures as the data set to improve robustness in the first experiment. The examples of all postures are shown in Fig. 16(a), and Fig. 16(b) shows the illustration of pressure distribution images. The ratio of the number of samples for each posture is approximately 1:0.5:0.5:1:1:1:1:1.

B. Short-term Experimental Results

Leave-One-Person-Out-Cross-Validation (LOPOCV) was used for data analysis. LOPOCV is a special case of cross-validation where the number of folds equals the number of subjects in the data set. In cross-validation, all data of one subject is used as the validation set, and the remaining data of other subjects are used as the training set for each fold. Therefore, the data of the same subject will not be included in the training set and validation set at the same time. It allows each subject to be used as a training set and test set, and get reliable results.

For neural network training, the relevant parameters are set as follows: the learning rate is 0.0001, the number of iterations for network training is 150, the batch size is 512, the optimization algorithm is adaptive moment estimation (Adam), the loss function is categorical cross-entropy, the momentum is 0.9 and the epsilon is 0.00001 for Batch Normalization.

Table I shows the posture classification accuracy of each subject. Table II summarizes the precision and recall results of 4 postures classification. The results show that the accuracy of posture classification is up to 95.08%.

TABLE II
CONFUSION MATRIX OF POSTURE CLASSIFICATION

		Ground Truth				
		Supine	Right	Left	Prone	Recall
Predicted	Supine	258	8	5	6	93.82%
	Right	5	256	8	0	95.17%
	Left	2	0	239	3	97.95%
	Prone	7	3	5	251	94.36%
	Precision	94.85%	95.88%	93.00%	96.54%	
Accuracy		95.08%				

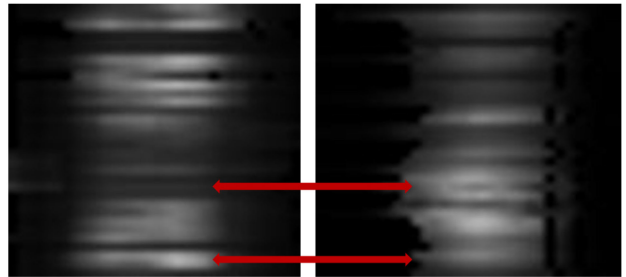


Fig. 17. Difference between supine and prone.

It is worth noting that supine and prone are easy to confuse because of the similar pressure distribution as shown in Fig. 17. In fact, compared with prone, the waist pressure on the mat is lower, and the hips pressure is higher in the supine. But this feature is difficult to accurately capture when the sensors of the mat have low density or insufficient accuracy. In our experiment, the results show that the accuracy of classification for supine and prone are 95.85% and 96.54% respectively. It proves that our mat system can accurately acquire the waist and hips pressure distribution.

Moreover, when the mat is placed in the middle of the bed and the width is about 1 m, people will not completely leave the scope of the mat when sleeping, which is still able to classify sleep postures. And the position of the body on the mat has little effect on posture classification because the mat is classified mainly by extracting the pressure distribution rather than position information.

TABLE III
THE ACCURACY OF CLASSIC NEURAL NETWORKS

Models	Model description	Accuracy
4-layer CNN	3 Conv + 3 MaxPool + 1 Fc	94.51%
AlexNet	5 Conv + 3 MaxPool + 3 Fc	94.79%
VGG-16	13 Conv + 5 MaxPool + 3 Fc	94.13%
GoogLeNet	21 Conv + 11 MaxPool + 3 Fc	92.80%
ResNet-18	17 Conv + 2 MaxPool + 3 Fc	95.08%

TABLE IV
CLASSIFICATION ACCURACY FOR DIFFERENT MODELS

Models	Model description	Accuracy
4-layer CNN	3 Conv + 3 MaxPool + 1 Fc	77.33%
ResNet-10	9 Conv + 2 MaxPool + 3 Fc	83.42%
VGG-16	13 Conv + 5 MaxPool + 3 Fc	85.59%
ResNet-18	17 Conv + 2 MaxPool + 3 Fc	86.35%

To compare with other neural networks, 4-layer CNN, AlexNet, VGG-16, and GoogLeNet, are also implemented for posture classification. The classification accuracy of these neural networks is summarized in Table III. Compare to other neural networks, ResNet-18 achieves the highest classification accuracy. In general, increasing the number of network layers can improve performance, but it may indirectly cause overfitting. ResNet solves this problem efficiently through residual blocks, which improves the performance for image classification.

C. Overnight Experimental Results

To evaluate the performance of the system in a real scenario, we conducted a whole night of continuous sleep data acquisition. Five subjects were included in the overnight experiment. The height of the subjects ranged from 168 to 185 cm, and the weight ranged from 60 to 87 kilograms. All the subjects in the overnight experiment did not participate in the short-term experiment. An infrared camera continuously recorded the ground truth postures. Since the subject did not move frequently when they sleep at night, the sampling frequency was decreased to 0.1Hz. After excluding the time of turning over, a total of 20521 pressure distribution images were acquired.

We used all data sets acquired in the first experiment as the training set and saved the model that converges after 300 iterations of training. Then the data of the second experiment was directly inputted into the model to obtain the classification results. The average accuracy of posture classification is up to 86.35%. Meanwhile, the “levels” of features can be enriched by the number of stacked layers. Table IV shows the classification accuracy for different models. ResNet-18 with the most layers achieves the highest classification accuracy.

Fig. 18 shows the posture classification results of one of the subjects, including the predicted and ground truth postures.

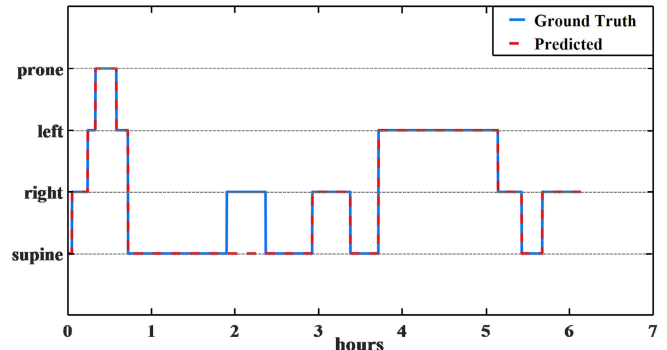


Fig. 18. Results of a 6 h overnight continuous acquisition with predicted and ground truth postures.

The subject's sleep postures changed 14 times a night, and the accuracy of posture classification is up to 92.99%.

According to the video of the overnight experiment, most of the postures are similar to 8 postures acquired in the short-term experiment. Thus, the short-term data set can represent the posture in most scenarios. It can be proved that our system can recognize sleep posture effectively in the real scenario, and has good robustness.

V. DISCUSSION

In this paper, a smart mat with high-density pressure sensor array is designed to provide a portable, non-intrusive, and comfortable way to identify the sleep postures is designed. Meanwhile, a neural network ResNet is applied to distinguish different sleep postures. The miniature scale mat combined with ResNet proved to provide adequate information for achieving satisfactory performance for sleep posture recognition.

In comparison with the existing works, Table V presents the studies that use an unobtrusive smart mat for sleep posture classification. As shown in Table V, some methods such as [24], [25] have yielded lower classification accuracy when compared to other methods. Some methods like [17], [19], [20], [26] have relatively high accuracy, but they don't classify supine and prone postures or have a relatively lower precision rate for supine and prone postures. Classification of these two postures is a mandatory step in pressure ulcer prevention because the tissues of the human body under pressure when prone is completely different from the supine. But as mentioned above, supine and prone are so similar that it is difficult to distinguish. This is why many methods don't identify the supine and prone as two separate classes.

There are also some methods that classify the supine and prone, and have obtained a high accuracy rate [18], [26], [27], [28]. But the area of the mat in these methods is very large (covering the entire bed) result in high production cost and pool portability. Meanwhile, these methods have a large number of sensors (even more than 8192) result in high computational complexity. Besides, the large area leads to lower sensor density such as in [18], which cannot acquire the local details such as the waist and hips pressure distribution.

TABLE V
COMPARISON OF THE PROPOSED METHOD WITH EXISTING METHODS M: TOTAL NUMBER OF SUBJECTS, N: TOTAL NUMBER OF SAMPLES, NA: NOT MENTIONED

Author, Year	Database	Sensor Type	Area and Sensor Density	Algorithms	Number of Postures Classified	Accuracy
Lower Classification Accuracy						
Mineharu <i>et al.</i> , 2015 [24].	M=10, N=270	1768 uniformly distributed pressure sensors,	0.51 m^2 , 0.35 $/cm^2$	Support vector machines	9	77.14%
Liu <i>et al.</i> , 2013 [25].	M=14, N=3360	8192 uniformly distributed FSR sensors	1.62 m^2 0.51 $/cm^2$	Minimum class residual classifier	6	83.02%
Supine and Prone Postures Are Not Distinguished Two Separate Classes or Prone Excluded						
Enokibori <i>et al.</i> , 2018 [26].	M=19, N=448	3200 uniformly distributed FSR sensors,	NA	Deep Neural Networks	3, prone excluded	99.7%
Huang <i>et al.</i> , 2017 [17].	M=NA, N=360	6 modules containing a matrix of FSR sensors each,	NA	Template matching by a minimum mean squared error	3, prone excluded	96.1%
Heydarzadeh <i>et al.</i> , 2016 [19].	M=10, N=NA	2048 uniformly distributed FSR sensors	1.62 m^2 (estimated) 0.13 $/cm^2$	Deep Neural Networks	3, prone excluded	98.06%
Pouyan <i>et al.</i> , 2013 [20].	M=20, N=160	2048 uniformly distributed FSR sensors	1.5 m^2 (estimated) 0.14 $/cm^2$	K nearest neighborhood	8, prone excluded	97.1%
Supine and Prone Postures Are Distinguished Two Separate Classes						
Matar <i>et al.</i> , 2020 [18].	M=12, N=1116	1728 uniformly distributed FSR sensors	1.41 m^2 0.12 $/cm^2$	Full connected networks	4	97.9%
Enokibori <i>et al.</i> , 2018 [26].	M=19, N=448	3200 uniformly distributed FSR sensors	NA	Deep Neural Networks	4	97.1%
Xu <i>et al.</i> , 2016 [27].	M=14, N=1848	8192 uniformly distributed FSR sensors	1.62 m^2 0.51 $/cm^2$	EMD+K nearest neighborhood	6	91.21%
Xu <i>et al.</i> , 2015 [28].	M=14, N=3360	8192 uniformly distributed FSR sensors	1.62 m^2 0.51 $/cm^2$	K nearest neighborhood	6	90.6%
Our method	M=16, N=1056	1024 uniformly distributed FSR sensors	0.30 m^2 0.34 $/cm^2$	ResNet	4	95.08%

Compared to other methods that classify the supine and prone, the area of the mat proposed in this paper is reduced by 80%-90%, and the number of sensors is also reduced by 40%-87.5%. Thus, the manufacturing costs are reduced by 50% approximately and the data processing complexity is also sharply decreased. In contrast, the portability is improved. Meanwhile, the sensor density of the mat has not decreased to ensure high classification accuracy. For example, the probability of confusion between the supine and prone is 2.4%. It proves that the waist and hips pressure distribution are acquired accurately by our mat system.

Not only has the hardware system improved, but we have also proposed a better algorithm for sleep posture recognition. Convolutional Neural Networks (CNN) has a good effect on image recognition because the convolution kernel can extract the different sizes of features accurately. As one of the most

common networks in CNN, the ResNet has solved the problems of gradient disappearance and explosion due to the increased network depth. Therefore, it increases the number of layers and improves the performance. For instance, the algorithm proposed in [18] is used for our data set, and the accuracy is just 92.52% as Table VI shows. It can be seen that this algorithm is still unable to accurately distinguish between supine and prone compare to our results. Meanwhile, since feature extraction is not required, it simplifies the algorithm and enables real-time monitoring on a low-power embedded computing platform. Therefore, it can be used for long-term continuous monitoring at home.

The mat proposed can still be enhanced by involving the following points. To our best knowledge, this paper was the first preliminarily study to verify the feasibility of using a miniature scale smart mat that only obtains the pressure distribution of major regions like the chest, part of the shoulders, and part

TABLE VI
POSTURE CLASSIFICATION RESULT WITH ALGORITHM PROPOSED IN [34]

Ground Truth					
Predicted	Supine	Right	Left	Prone	Recall
Supine	252	8	8	13	89.68%
	Right	3	250	0	97.28%
	Left	6	1	239	94.45%
	Prone	11	8	10	236
	Precision	92.65%	93.63%	93.00%	90.77%
Accuracy		92.52%			

of the hips to achieve favorable performance for sleep posture recognition. While, if the bed is wider such as a double bed, the major regions that we expect to monitor may be outside of the mat. Therefore, in the future, for a double bed, the length of the mat will be increased to ensure the major regions of the body can be measured. Meanwhile, currently, only the press distribution was obtained, while, the respiration rate can also be measured through the mat. Hence, in the future, the respiration rate will also be included to enrich the functionality of the smart mat system.

VI. CONCLUSION

In this paper, for offering an unobtrusive, comfortable, and high-resolution solution for sleep postures monitoring, a miniature scale with a five-layer structure and 1024 flexible pressure sensors is designed. Meanwhile, an algorithmic framework including pre-processing and ResNet that doesn't require the complex hand-crafted feature extraction process is used to distinguish different postures. Experimental results show that the accuracy of the short-term experiment is up to 95.08%, and the accuracy of the overnight is up to 86.35%. Compare to other methods, our system can achieve a satisfactory classification accuracy while reducing the area of the mat and the number of sensors, which potentially reduce the cost and computational complexity and increase the portability. Moreover, the mat system can still be enhanced by exploring and integrating other information, like breathing and body movements, to provide a more comprehensive evaluation of sleep. Meanwhile, it can monitor the transition effect and the process of change by adding sensors and increasing sampling frequency in the future.

REFERENCES

- [1] J. M. Parish, "Sleep-Related problems in common medical conditions," *Chest*, vol. 135, no. 2, pp. 563–572, Feb. 2009.
- [2] M. E. Thase, "Depression and sleep: Pathophysiology and treatment," *Dialogues Clin. Neurosci.*, vol. 8, no. 2, pp. 217–226, 2006.
- [3] J. H. Lee and W. C. Wong, "Approximate dynamic programming approach for process control," *IFAC Proc. Vol.*, vol. vol. 42, no. 11, pp. 26–35, Jan. 2009.
- [4] C. Ambrogio, X. Lowman, M. Kuo, J. Malo, A. R. Prasad, and S. Parthasarathy, "Sleep and non-invasive ventilation in patients with chronic respiratory insufficiency," *Intensive Care Med*, vol. 35, no. 2, pp. 306–313, Sep. 2008.
- [5] A. Oksenberg and D. S. Silverberg, "The effect of body posture on sleep-related breathing disorders: Facts and therapeutic implications," *Sleep Med. Rev.*, vol. 2, no. 3, pp. 139–162, Aug. 1998.
- [6] R. Winsky-Sommerer, P. de Oliveira, S. Loomis, K. Wafford, D.-J. Dijk, and G. Gilmour, "Disturbances of sleep quality, timing and structure and their relationship with other neuropsychiatric symptoms in Alzheimer's disease and schizophrenia: Insights from studies in patient populations and animal models," *Neurosci. Biobehav. Rev.*, vol. 97, pp. 112–137, Feb. 2019.
- [7] H. Brem *et al.*, "High cost of stage IV pressure ulcers," *Am. J. Surg.*, vol. 200, no. 4, pp. 473–477, Oct. 2010.
- [8] L. M. Soban, S. Hempel, B. A. Munjas, J. Miles, and L. V. Rubenstein, "Preventing pressure ulcers in hospitals: A systematic review of nurse-focused quality improvement interventions," *Jt. Comm. J. Qual. Patient Saf.*, vol. 37, no. 6, pp. 245–AP16, Jun. 2011.
- [9] L. Nuksawn, E. Nantajeewarawat, and S. Thiemjarus, "Real-time sensor- and camera-based logging of sleep postures," in *Proc. Int. Comput. Sci. Eng. Conf.*, 2015, pp. 1–6.
- [10] W.-H. Liao and C.-M. Yang, "Video-based activity and movement pattern analysis in overnight sleep studies," in *Proc. 19th Int. Conf. Pattern Recognit.*, 2008, pp. 1–4.
- [11] X. Dai, *Vision-Based 3D Human Motion Analysis For Fall Detection and Bed-Exiting*. University Of Denver, 2013.
- [12] M. Chang *et al.*, "Multimodal sensor system for pressure ulcer wound assessment and care," *IEEE Trans. Ind. Informat.*, vol. 14, no. 3, pp. 1186–1196, Mar. 2018.
- [13] W. Liao and C. Yang, "Video-based activity and movement pattern analysis in overnight sleep studies," in *Proc. 19th Int. Conf. Pattern Recognit.*, Dec. 2008, pp. 1–4.
- [14] P. Jiang and R. Zhu, "Dual tri-axis accelerometers for monitoring physiological parameters of human body in sleep," in *Proc. IEEE SENSORS*, Orlando, FL, USA, 2016, pp. 1–3.
- [15] A. Kitzig, E. Naroska, G. Stockmanns, R. Viga, and A. Grabmaier, "A novel approach to creating artificial training and test data for an HMM based posture recognition system," in *Proc. IEEE 26th Int. Workshop Mach. Learn. Signal Process.*, Sep. 2016, pp. 1–6.
- [16] S. Lokavee, N. Watthanawisuth, J. P. Mensing, and T. Kerdcharoen, "Sensor pillow system: Monitoring cardio-respiratory and posture movements during sleep," in *Proc. 4th 2011 Biomed. Eng. Int. Conf.*, Jan. 2012, pp. 71–75.
- [17] Y.-F. Huang *et al.*, "An improved sleep posture recognition based on force sensing resistors," in *Proc. Intell. Inf. Database Syst.*, Cham, 2017, pp. 318–327.
- [18] G. Matar, J.-M. Lina, and G. Kaddoum, "Artificial neural network for in-Bed posture classification using bed-sheet pressure sensors," *IEEE J. Biomed. Health Inform.*, vol. 24, no. 1, pp. 101–110, Jan. 2020.
- [19] M. Heydarzadeh, M. Nourani, and S. Ostadabbas, "In-bed posture classification using deep autoencoders," in *Proc. 38th Annu. Int. Conf. IEEE Eng. Med. Biol. Soc.*, Aug. 2016, pp. 3839–3842.
- [20] M. B. Pouyan, S. Ostadabbas, M. Farshbaf, R. Yousefifi, M. Nourani, and M. D. M. Pompeo, "Continuous eight-posture classification for bed-bound patients," in *Proc. 6th Int. Conf. Biomed. Eng. Inform.*, Dec. 2013, pp. 121–126.
- [21] W. Li, C. Sun, W. Yuan, W. Gu, Z. Cui, and W. Chen, "Smart mat system with pressure sensor array for unobtrusive sleep monitoring," in *Proc. 39th Annu. Int. Conf. IEEE Eng. Med. Biol. Soc.*, 2017, pp. 177–180.
- [22] K. He, X. Zhang, S. Ren, and J. Sun, "Deep residual learning for image recognition," in *Proc. IEEE Conf. Comput. Vis. Pattern Recognit.*, Jun. 2016, pp. 770–778.
- [23] C. Idrzikowski, *Beating Insomnia: How to Get a Good Night's Sleep*. Gill & MacMillan, 2003.
- [24] A. Mineharu, N. Kuwahara, and K. Morimoto, "A study of automatic classification of sleeping position by a pressure-sensitive sensor," in *Proc. Int. Conf. Inform., Electron. Vis.*, Jun. 2015, pp. 1–5.
- [25] J. J. Liu *et al.*, "Sleep posture analysis using a dense pressure sensitive bedsheet," *Pervasive Mob. Comput.*, vol. 10, pp. 34–50, Feb. 2014.
- [26] Y. Enokibori and K. Mase, "Data augmentation to build high performance DNN for in-bed posture classification," *J. Inf. Process.*, vol. 26, pp. 718–727, 2018.
- [27] X. Xu, F. Lin, A. Wang, Y. Hu, M.-C. Huang, and W. Xu, "Body-Earth mover's distance: A matching-based approach for sleep posture recognition," *IEEE Trans. Biomed. Circuits Syst.*, vol. 10, no. 5, pp. 1023–1035, Oct. 2016.
- [28] X. Xu, F. Lin, A. Wang, C. Song, Y. Hu, and W. Xu, "On-bed sleep posture recognition based on body-earth mover's distance," in *Proc. IEEE Biomed. Circuits Syst. Conf.*, Oct. 2015, pp. 1–4.



Haikang Diao received the B.Eng. degree in electronic engineering from Fudan University, Shanghai, China, in 2019, where he is currently working toward the M.Sc. degree with the Center for Intelligent Medical Electronics, Department of Electronic Engineering, School of Information Science and Technology. His research interests include biomedical sensing technology, sleep posture recognition, and artificial intelligence for health care.



monitoring.

Chen Chen received the M.S. degree in embedded system from Institut Supérieur d'Électronique de Paris, Paris, France, in 2013 and the Ph.D. degree in computer science from Université Pierre et Marie Curie (UPMC) in 2016. She is a Postdoctoral Researcher with the Centre of Intelligent Medical Electronics, School of Information Science and Technology, Fudan University, Shanghai, China. Her research interests include biomedical engineering, focusing on wearable sensor systems, biomedical signal processing, sleep analysis, and personalized health



Wei Yuan received the Ph.D. degree in textile engineering from Soochow University, Suzhou, China, in 2014. After two year Postdoctoral Research with Suzhou Institute of Nano-Tech and Nano-Bionics (SINANO), Chinese Academy of Sciences, he is currently an Assistant Research Fellow with Printable Electronics Research Center (PERC) of SINANO. He has authored or coauthored more than 10 technical publications in international journals as the first author or corresponding author, such as *ACS Appl. Mater. Interface*, *Langmuir*, *Journal of semiconductor*, *RSC Advances*, and authored or coauthored more than five patents. His current research interests include preparing flexible and stretchable electronics based on textile fabrics, all-printed large-scale electroluminescence devices on fabrics, high mechanical strength printed electrodes on fabrics, and stretchable smart textiles.



Amara Amara (Senior Member, IEEE) received the master's degree in microelectronics and computer science and the Ph.D. degree in computer science from Paris VI University, Paris, France, in 1984 and 1989, respectively. After 3 years as an Assistant Professor with Paris VI University, he joined IBM research and development laboratory with Corbeil Essonne as a Visiting Researcher, where he was involved in SRAM memory design with advanced CMOS technologies. In 1992, he joined ISEP (Paris Institute for Electronics), where he was the Head of the microelectronics laboratory. He was then appointed in 2006 Deputy Managing Director of ISEP in charge of Research and International Cooperation up to March 2017. His research interests include low power circuit design techniques and on design and technology interaction for advanced technologies (SOI, DGates FD SOI, Ultra-Thin Body SOI, and 3D Integration). He is currently more involved on how to use advanced technologies such as artificial intelligence and blockchain to help solving health issues in low income countries.



Toshiyo Tamura (Life Member, IEEE) received the Ph.D. degree from Tokyo Medical and Dental University, Tokyo, Japan, in 1980. He is currently a Visiting Professor, Future Robotics Organization, Waseda University, Tokyo, Japan. His research interests include biomedical instrumentation, biosignal processing, telemedicine telecare, home care technology, and rehabilitation engineering. He and his colleagues book entitled "*Biomedical sensors and instruments*" and "*Seamless healthcare monitoring*" are popular textbooks for bioinstrumentation and medical devices. He also wrote several chapters including sensors for telemedicine and application of wearable inertia sensors. He has been involved regional innovation strategy support program and creates innovations for achieving healthy and long life through the development of health care systems with smart bioinstrumentation and testing. He has developed unobtrusive monitoring systems and wearable devices for improving the quality of life.



monitoring.

Jiahao Fan received the B.S. degree in communication engineering and M.S. degree in electronic and communication engineering from Jilin University, Changchun, China, in 2013 and 2016, respectively. He is currently working toward the Ph.D. degree with Center for Intelligent Medical Electronics, the Department of Electronic Engineering, School of Information Science and Technology, Fudan University, Shanghai, China. His research interests focuses on sleep related algorithms, which mainly are automatic stage scoring and sleep disease detection.

Long Meng received the B.S. degree in applied physics from Northeastern University, Shenyang, China, in 2011 and the M.S. degree in circuits and systems from Fudan University, Shanghai, China, in 2018. He is currently working toward the Ph.D. degree with the Centre of Intelligent Medical Electronics, School of Information Science and Technology, Fudan University. His research interests include biomedical engineering, focusing on wearable sensor systems, biomedical signal processing, stroke assessment and rehabilitation, and personalized health



Xiangyu Liu received the master's degree from East China University of Science and Technology (The Design Methodology), Shanghai, China, where he is currently working toward the Ph.D. degree. He is currently an Industrial Designer with the Center of Intelligent Medical Electronics, School of Information Science and Technology, Fudan University, Shanghai, China. His main research interests includeneuromuscular control mechanisms and prosthesis control.

Wei Chen (Senior Member, IEEE) received the B.Eng. and M.Eng. degrees from the School of Electronics and Information Engineering, Xi'an Jiaotong University, Xi'an, China, in 1999 and 2002, respectively, and the Ph.D. degree from the Department of Electrical and Electronics Engineering, University of Melbourne, Melbourne, VIC, Australia, in 2007. She took an Internship with Bell Laboratories, Alcatel-Lucent, Stuttgart, Germany, in 2005, and she was a Research Assistant with the Department of Electrical and Electronics Engineering, University of Melbourne, Australia, in 2007. Since October 2015, she has been a Full Professor and the Director of the Center for Intelligent Medical Electronics (CIME), Department of Electronic Engineering, School of Information Science and Technology, Fudan University, Shanghai, China. Her research interests include patient health monitoring, medical monitoring system design using wearable sensors, sleep monitoring, brain activity monitoring, wireless body area networks, ambient intelligence, personalized and smart environment, smart sensor systems, and signal processing.